ACS APPLIED MATERIALS & INTERFACES

Research Article

www.acsami.org

Effects of Ionic Liquid Molecules in Hybrid PbS Quantum Dot–Organic Solar Cells

Gi-Hwan Kim, Hak-Beom Kim, Bright Walker, Hyosung Choi, Changjin Yang, Jongnam Park,* and Jin Young Kim*

Interdisciplinary School of Green Energy and KIER-UNIST Advanced Center for Energy, Ulsan National Institute of Science and Technology (UNIST), Ulsan 689-798, South Korea

Supporting Information

ABSTRACT: We investigated the effect of ionic liquid molecules (ILMs) in hybrid quantum dot-organic solar cells (HyQD-OSCs). The insertion of an ILM layer between PbS and phenyl-C61-butyric acid methyl ester (PCBM) can shift the band edge of PCBM closer to the vacuum level of PbS due to spontaneous dipole polarization. Because of this new architecture, improvements in device performance were achieved, including increases in open-circuit voltage (V_{OC}, from 0.41 V to 0.49 V), fill factor (FF, from 0.48 to 0.59), and power conversion efficiency (PCE, from 1.62% to 2.21%), compared to reference devices under AM 1.5G illumination at 100 mW cm^{-2}. We observed that treatment of the PbS layer with ILMs causes a significant increase in work function from 3.58 eV to 3.93 eV. Furthermore, the ILMs layer minimizes the contact resistance between PbS and PCBM due to the improved compatibility between the two layers, confirmed as a decrease in charge transfer resistance, as measured by electrical impedance spectroscopy.

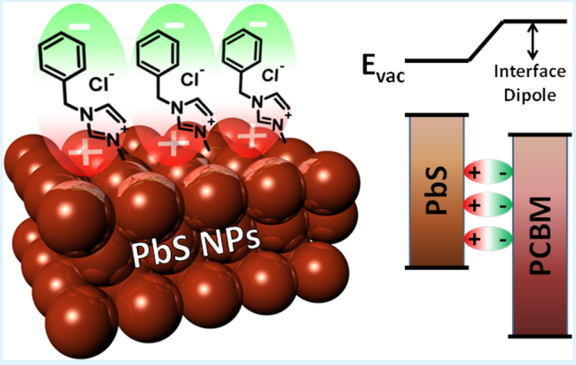

KEYWORDS: *photovoltaics, hybrid solar cells, quantum dots, quantum dot solar cells, PbS, ionic liquid molecules*

1. INTRODUCTION

In the last few decades, significant research attempts have been undertaken to develop large-area, flexible, low-cost, and high power conversion efficiency (PCE) photovoltaic devices through the use of nanostructured materials, including small molecules, conjugated polymers, and colloidal nanocrystal quantum dots (QDs).[1−7] QDs have attracted interest in the development of solar cells due to their unique features. These include size-dependent optical absorption spectra, large extinction coefficients and extended photostability, which make them attractive absorbing materials in photovoltaic applications. QDs also offer the intriguing possibility of overcoming the ordinary thermodynamic limits of solar energy conversion, if multiple or hot charge carriers can be extracted.[6−14]

Recently, extensive research has focused on the use of lead chalcogenide nanocrystals (PbS and PbSe) to harvest infrared (IR) light with wavelengths beyond 1000 nm.[8−11] In addition, nanocrystals of these low-band-gap materials have demonstrated multiple exciton generation, which can potentially provide efficient use of the ultraviolet (UV) region of the solar spectrum.[12−15] However, the band gap of a PbS QD must be near 1.3 eV in order to achieve proper band alignment with acceptor materials in this type of hybrid heterojunction solar cell.[16−18] In organic solar cells, the open-circuit voltage (V_{OC}) is limited by the difference in the energy between the highest occupied molecular orbital (HOMO) level of the donor and lowest unoccupied molecular orbital (LUMO) level of the acceptor.[2−5] Therefore, the relatively high HOMO level of the donor (PbS and PbSe QDs) and low LUMO level of the acceptor (TiO_2, ZnO, and phenyl-C61-butyric acid methyl ester (PCBM)) limit the V_{OC} and PCE of PbS QD solar cells, compared to other compound inorganic solar cells. To overcome this issue in QD solar cells (QD-SCs), the study of interface engineering between the donor and the acceptor provides valuable insight toward improving the V_{OC} and PCE of hybrid quantum dot−organic solar cells (HyQD-OSCs).

In this study, we observed a remarkable improvement in HyQD-OSCs performance, including increases in V_{OC} from 0.41 to 0.49 V, fill factor (FF) from 0.48 to 0.59, and PCE from 1.62% to 2.21%, via the incorporation of ILMs. We find that 1-benzyl-3-methylimidazolium chloride (BenMeIm-Cl) forms a spontaneously oriented dipole at the donor/acceptor interface, acting as a vacuum level tuning layer.[20−22]

2. EXPERIMENTAL SECTION

2.1. Materials. PbS nanoparticles were synthesized by adding lead oxide (PbO, 99.99%, Sigma−Aldrich) (0.47 g), oleic acid (OA, tech. grade 90%, Sigma−Aldrich) (2 g), and 1-octadecene (ODE, tech. grade 90%, Sigma−Aldrich) (10 g) to a three-neck round-bottom flask.

Received: December 5, 2012
Accepted: February 12, 2013
Published: February 12, 2013

   dx.doi.org/10.1021/am3029766 | ACS Appl. Mater. Interfaces 2013, 5, 1757−1760

The mixture was heated to 120 °C under vacuum for 1 h and then kept under argon. In a glovebox, hexamethyldisilathiane (synthesis grade, Sigma–Aldrich) (180 μL) was mixed with octane (grade 99%, Sigma–Aldrich) (5 mL) and loaded into a syringe. The contents of the syringe were quickly injected into the flask, the heating mantle was removed after 1 min, and the PbS nanoparticles were cooled to room temperature. The reaction solution was mixed with hexane (10 mL), ethanol (10 mL), and acetone (10 mL) and centrifuged to isolate the PbS nanoparticles. This washing step was repeated several times.

2.2. Device Fabrication. Poly(3,4-ethylenedioxythiophene):poly-(4-styrenesulfonate) (PEDOT:PSS) and PCBM were purchased from H.C. Starck (Germany) and Electronic Materials (EM) Index Co., Inc., respectively. PEDOT:PSS was spin-coated onto a indium tin oxide (ITO)-coated glass substrate at 5000 rpm for 60 s and then baked at 140 °C for 10 min in air. The PbS nanoparticle layer was sequentially spin-coated using a 10 mg mL^{-1} solution in chlorobenzene (CB) at 1000 rpm for 60 s. The ligands of QD layer were next exchanged by immersing the device into a solution of 0.01 M ethanedithiol (EDT) in acetonitrile for 1 min, then rinsed with acetonitrile and chlorobenzene at 1000 rpm for 60 s. Subsequent nanoparticle layers were deposited by repeatedly spin-coating the NP solution and repeating the ligand exchange and rinsing steps until the desired thickness of the donor layer was achieved. The highest performance of HyQD-OSCs were obtained from devices with a PbS thickness of 160 nm, prepared by repeating the coating procedure 8 times. An ionic liquid solution, BenMeIm-Cl dissolved in methanol (0.1 wt %) was spin-coated at 5000 rpm for 60 s on the PbS layer and then annealed at 100 °C for 10 min to remove residual methanol. A solution of PCBM dissolved in CB (1 wt %) was spin-coated at 1000 rpm for 60 s. Finally, the device was pumped down in vacuum ($<10^{-7}$ Torr; 1 Torr ≈ 133 Pa) and a 100-nm-thick Al electrode was deposited on top of the PCBM layer by thermal evaporation at a rate of ∼1 Å/s. The deposited Al electrode area defined the active area of the devices as 13 mm^2.

2.3. Measurement. Samples were illuminated using a xenon arc lamp with a KG filter calibrated at 100 mW/cm^2 with an NREL certified silicon photodiode. A Keithley Model 2400 source measure unit was used to collect current density–voltage (J–V) curves. Ultraviolet–infrared–near-infrared (UV-vis-NIR) absorption spectra were measured on a Varian Cary 5000 spectrophotometer. The sizes of the PbS QDs were measured by high-resolution transmission electron microscopy (HRTEM) using a JEM-2100F (Cs corrector) HR-TEM system. The elemental composition of the PbS/ILMs films were characterized by X-ray photoelectron spectroscopy (XPS) (K-alpha, Thermo Fisher). External quantum efficiency (EQE) measurements were obtained under ambient conditions using a PV Measurements OE system in which monochromated light from a xenon lamp was chopped at 100 Hz and photocurrent was measured using a lock-in amplifier and compared to a reference silicon photodiode.

3. RESULTS AND DISCUSSION

In order to study the effect of ionic liquids on HyQD-OSCs, PbS QDs were synthesized using slight modifications to a previously reported procedure,[18] as described in the Experimental Section. PbS QDs were then characterized by UV-vis-NIR absorption spectroscopy as well as HRTEM. The absorption spectrum is shown in Figure 1a, exhibiting a first excitonic transition at λ = 950 nm (1.3 eV). Figure 1b shows the size of the PbS QDs to be ∼3.6–3.9 nm. From both the absorption peak and size distribution, the band gap of PbS nanoparticles was determined to be 1.2–1.3 eV,[18] within a range which is suitable for use as the absorbing material in QD-SCs.

To investigate the effect that ILMs have on the electronic properties of PbS QD films, ultraviolet photoelectron spectra (UPS) were collected for PbS films with and without ILMs treatment. We observed that treatment with ILMs on PbS layer

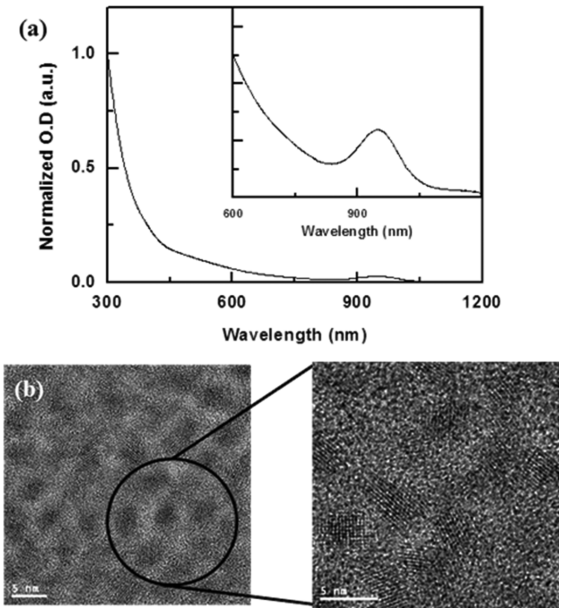

Figure 1. (a) UV-vis-NIR absorption spectra. Inset: magnified absorbance spectrum in the range of 600–1200 nm. (b) HRTEM image (scale bar = 5 nm in both micrographs) of PbS nanoparticles deposited from a dilute hexane solution.

causes a significant increase in work function of the PbS layer from 3.58 eV to 3.93 eV, as measured by UPS, using HeI emission ($h\nu$ = 21.2 eV) as a light source (Figure 2).[19] The work function was calculated via the relationship between the incident photon energy ($h\nu$) and the secondary edge position (E_{SE}), as described in eq 1:

$$\mathrm{WF} = h\nu - E_{SE} \quad (1)$$

Figure 3 schematically illustrates the energy band diagram (flat band condition) of HyQD-OSCs with and without ILMs modification. Insertion of ILMs between the donor and the acceptor causes a shift in the vacuum level, implying the formation of an interfacial dipole within the layer, as illustrated in Figure 3a.[20,22] The N and Cl peaks of ILMs were observed in XPS survey spectrum, as shown in Figure S1 in the Supporting Information, consistent with the presence of BenMeIm-Cl at the PbS surface. It may be expected that the BenMeIm-Cl cations are attracted to the sulfide/sulfur atoms in the PbS layer, while Cl^- anions move toward the PCBM surface. This spontaneously oriented interfacial layer leads to the formation of a permanent dipole oriented from the PCBM toward the PbS phase. Figure 3b illustrates that when the spontaneously oriented dipoles are pointing away from the PCBM, the band edge of the PCBM shifts closer to the vacuum level of the PbS layer.[20−23] These changes in band structure have a positive impact on device properties, allowing the V_{OC} to increase markedly by enlarging the energy level difference between the HOMO level of PbS and LUMO level of PCBM.

Figure 4a shows the current density versus voltage (J–V) characteristics of the PbS/PCBM HyQD-OSCs with and without ILMs measured under AM 1.5G illumination at 100 mW cm^{-2}. The photovoltaic characteristics are summarized in Table 1. While the device without ILMs shows a short-circuit current density (J_{SC}) of 8.24 mA cm^{-2} and values of V_{OC} = 0.41 V, FF = 0.48, and PCE = 1.62%, the device with ILMs displays values of J_{SC} = 7.63 mA cm^{-2}, V_{OC} = 0.49 V, FF = 0.59, and PCE = 2.21%. The noticeable enhancement of HyQD-OSCs

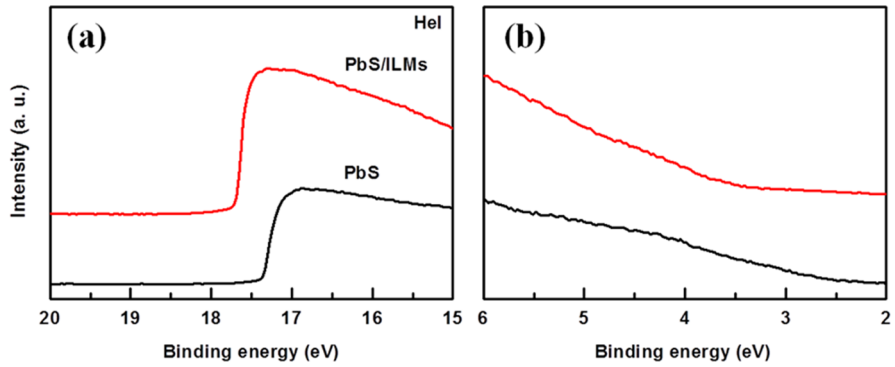

Figure 2. Ultraviolet photoemission spectroscopy (UPS) spectra of PbS and PbS/ILMs films: (a) secondary edge region and (b) HOMO region. The calculated work functions of PbS and PbS/ILMs are 3.58 and 3.93 eV, respectively.

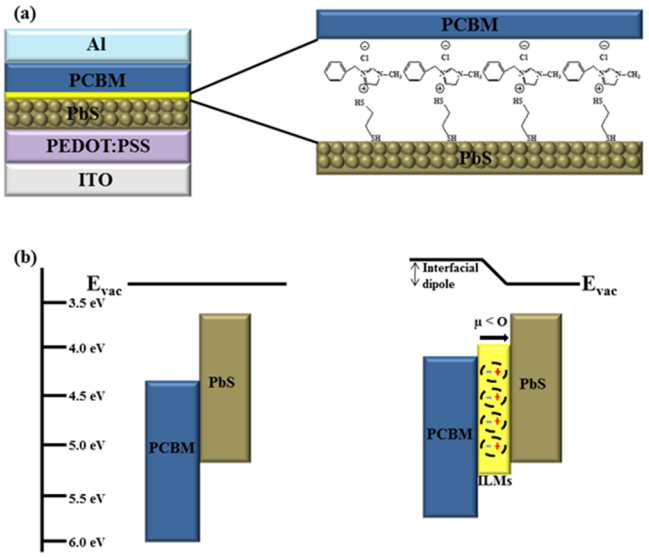

Figure 3. (a) Device architecture of PbS/PCBM HyQD-OSCs with ILMs layer. (b) Schematic energy diagrams for flat band condition without and with an ILM layer.

performance is derived from enhanced values of V_{OC} and FF, compared to those of the reference device parameters. V_{OC} enhancement is attributed to the shift of the band edge of the PCBM, closer to the vacuum level of PbS, because of the spontaneous dipole polarization within the ILMs layer. The J_{SC} value of the device with ILMs is slightly lower than that of the reference device. It is possible that the ILM layer acts as a thin dielectric layer, separating the PbS and PCBM phases, thereby inhibiting charge transfer, relative to the reference device.

Table 1. Device Characteristics of PbS/PCBM Solar Cells with and without an ILM Layer

property	PbS/PCBM	PbS/ILMs/PCBM
short-circuit current density, J_{SC} (mA cm^{-2})	8.24 (±0.12)	7.63 (±0.15)
open-circuit voltage, V_{OC} (V)	0.41 (±0.02)	0.49 (±0.02)
fill factor, FF	0.48 (±0.03)	0.59 (±0.03)
power conversion efficiency, PCE (%)	1.62 (±0.14)	2.21 (±0.12)
series resistance, R_S (Ω cm^2)	12.42	9.29
shunt resistance, R_{Sh} (Ω cm^2)	205.23	723.46

Therefore, a lower J_{SC} value might be expected from the device with ILMs, compared to the reference device. The observed J_{SC} values are in agreement with the J_{SC} values obtained via integration of the EQE spectrum (Figure 4b). As expected, the features observed in the EQE fit the absorption spectrum of the PbS nanoparticles, including an onset at ∼1050 nm, a local maximum at ∼950 nm (corresponding to the first excitonic transition), a local minimum at ∼850 nm, and a gradual increase in intensity at shorter wavelengths, as shown in Figure 1a.

In addition, the ILMs layer minimizes the contact resistance between PbS and PCBM, because of the improved compatibility between the two layers, as confirmed by electrical impedance spectroscopy[22,24] (see Figure 5). Cole−Cole plots were collected for optimized devices with and without ILM layers under illumination (100 mW cm^{-2}) at the V_{OC} condition. The charge-transfer resistance (R_{CT}) measured for the devices under illumination was found to decrease from 10.54 Ω cm^2 to 8.81 Ω cm^2 upon incorporation of the ILMs. This decrease in R_{CT} has previously been associated with an increase in FF and

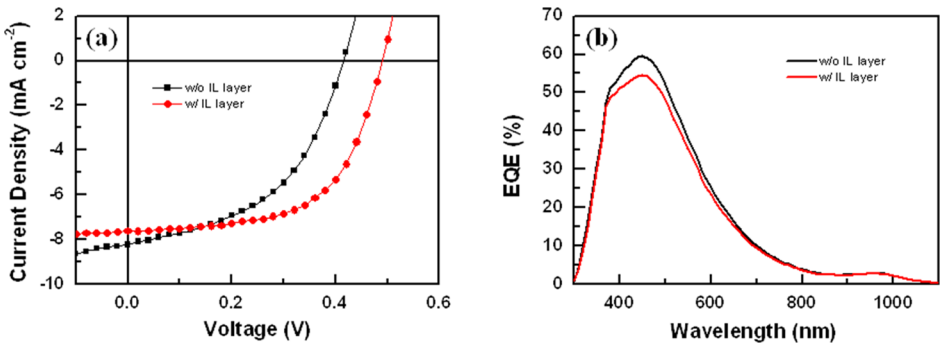

Figure 4. (a) $J-V$ characteristics and (b) EQE of PbS/PCBM hybrid quantum dot solar cells with and without an ILM layer.

dx.doi.org/10.1021/am3029766 | ACS Appl. Mater. Interfaces 2013, 5, 1757−1760

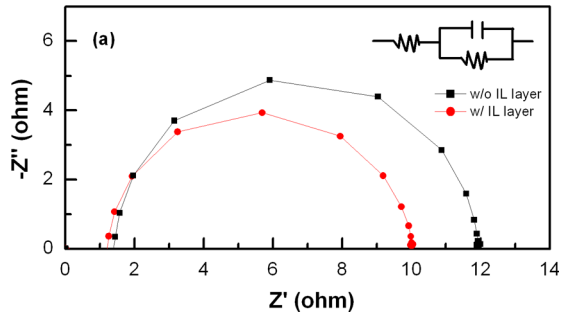

Figure 5. Electrical impedance spectra for PbS:PCBM hybrid quantum dot–organic solar cells (HyQD-OSCs) with and without the ILM layer under illumination (100 mW cm^{-2}). Inset shows the equivalent circuit of the device.

PCE.[22,24,25] The increased FF and PCE values, from 0.48 to 0.59 and 1.62% to 2.21%, respectively, upon incorporation of the ILMs layer are consistent with the R_S and R_{Sh}, as measured from $J-V$ curves (Figure 4a), which show a decrease in R_S from 12.42 Ω cm^2 to 9.29 Ω cm^2 and increases in shunt resistance (R_{Sh}) from 205.23 Ω cm^2 to 723.56 Ω cm^2 from the devices.

CONCLUSIONS

In summary, we have demonstrated a significant increase in performance in hybrid quantum dot–organic solar cells (HyQD-OSCs) through the incorporation of an ionic liquid molecule (ILM) layer. The incorporation of the ILM layer consisting of imidazolium cations and Cl^- anions between PbS nanoparticles and PCBM layers is found to shift the band edge of PCBM closer to the vacuum level of the PbS due to spontaneous dipole formation. This change in band structure has a positive effect on device performance, leading to an increase in open-circuit potential (V_{OC}) from 0.41 to 0.49 V, an increase in fill factor (FF) from 0.48 to 0.59 and an increase in power conversion efficiency (PCE) from 1.62% to 2.21%. This outstanding enhancement of HyQD-OSCs demonstrates that interface engineering and the incorporation of ILMs layers can offer a strategy to overcome the low V_{OC} typically observed in the HyQD-OSCs.

ASSOCIATED CONTENT

Supporting Information

Data from X-ray photoelectron spectroscopy and electrical impedance measurements. This material is available free of charge via the Internet at http://pubs.acs.org.

AUTHOR INFORMATION

Corresponding Author

*Tel.: +82-52-217-2911. Fax: +82-52-217-2909. E-mail addresses: jykim@unist.ac.kr (J.Y.K.), jnpark@unist.ac.kr (J.P.).

Notes

The authors declare no competing financial interest.

ACKNOWLEDGMENTS

This research was supported by NRF Korea (Nos. WCU/R31-2008-000-20012-0 and 2010-0007431), and by the Basic Science Research Program through the National Research Foundation of Korea (NRF) funded by the Ministry of Education, Science and Technology (No. 2011-0014688).

REFERENCES

(1) Tang, C. *Appl. Phys. Lett.* **1986**, *48*, 183–185.
(2) Peumans, P.; Uchida, S.; Forrest, S. R. *Nature* **2003**, *425*, 158–162.
(3) Kim, J. Y.; Lee, K.; Coates, N. E.; Moses, D.; Nguyen, T. Q.; Dante, M.; Heeger, A. J. *Science* **2007**, *317*, 222–225.
(4) Park, S. H.; Roy, A.; Beaupre, S.; Cho, S.; Coates, N.; Moon, J. S.; Moses, D.; Leclerc, M.; Lee, K.; Heeger, A. J. *Nat. Photon.* **2009**, *3*, 297–302.
(5) Chen, H. Y.; Hou, J.; Zhang, S.; Liang, Y.; Yang, G.; Yang, Y.; Yu, L.; Wu, Y.; Li, G. *Nat. Photon.* **2009**, *3*, 649–653.
(6) Alivisatos, A. P. *Science* **1996**, *271*, 933–937.
(7) Gur, I.; Fromer, N. A.; Geier, M. L.; Alivisatos, A. P. *Science* **2005**, *310*, 462–465.
(8) Watt, A. A. R.; Blake, D.; Warner, J. H.; Thomsen, E. A.; Tavenner, E. L.; Rubinsztein-Dunlop, H.; Meredith, P. *J. Phys. D: Appl. Phys.* **2005**, *38*, 2006–2012.
(9) McDonald, S. A.; Konstantatos, G.; Zhang, S.; Cyr, P. W.; Klem, E. J. D.; Levina, L.; Sargent, E. H. *Nat. Mater.* **2005**, *4*, 138–142.
(10) Zhang, S.; Cyr, P.; McDonald, S.; Konstantatos, G.; Sargent, E. *Appl. Phys. Lett.* **2005**, *87*, 233101.
(11) Luther, J. M.; Law, M.; Beard, M. C.; Song, Q.; Reese, M. O.; Ellingson, R. J.; Nozik, A. J. *Nano Lett.* **2008**, *8*, 3488–3492.
(12) Klimov, V.; Mikhailovsky, A.; McBranch, D.; Leatherdale, C.; Bawendi, M. *Science* **2000**, *287*, 1011–1013.
(13) Kim, S. J.; Kim, W. J.; Sahoo, Y.; Cartwright, A. N.; Prasad, P. N. *Appl. Phys. Lett.* **2008**, *92*, 031107.
(14) Rauch, T.; Boberl, M.; Tedde, S. F.; Furst, J.; Kovalenko, M. V.; Hesser, G.; Lemmer, U.; Heiss, W.; Hayden, O. *Nat. Photon.* **2009**, *3*, 332–336.
(15) Sukhovatkin, V.; Hinds, S.; Brzozowski, L.; Sargent, E. H. *Science* **2009**, *324*, 1542–1544.
(16) Pattantyus-Abraham, A. G.; Kramer, I. J.; Barkhouse, A. R.; Wang, X.; Konstantatos, G.; Debnath, R.; Levina, L.; Raabe, I.; Nazeeruddin, M. K.; Gratzel, M. *ACS Nano* **2010**, *4*, 3374–3380.
(17) Hyun, B. R.; Zhong, Y. W.; Bartnik, A. C.; Sun, L.; Abruña, H. D.; Wise, F. W.; Goodreau, J. D.; Matthews, J. R.; Leslie, T. M.; Borrelli, N. F. *ACS Nano* **2008**, *2*, 2206–2212.
(18) Luther, J. M.; Gao, J.; Lloyd, M. T.; Semonin, O. E.; Beard, M. C.; Nozik, A. J. *Adv. Mater.* **2010**, *22*, 3704–3707.
(19) Seo, J. H.; Yang, R.; Brzezinski, J. Z.; Walker, B.; Bazan, G. C.; Nguyen, T. Q. *Adv. Mater.* **2009**, *21*, 1006–1011.
(20) Lee, B. R.; Choi, H.; Sun Park, J.; Lee, H. J.; Kim, S. O.; Kim, J. Y.; Song, M. H. *J. Mater. Chem.* **2011**, *21*, 2051–2053.
(21) Goh, C.; Scully, S. R.; McGehee, M. D. *J. Appl. Phys.* **2007**, *101*, 114503.
(22) Choi, H.; Park, J. S.; Jeong, E.; Kim, G. H.; Lee, B. R.; Kim, S. O.; Song, M. H.; Woo, H. Y.; Kim, J. Y. *Adv. Mater.* **2010**, *12*, 15309–15314.
(23) Choi, H.; Cho, H.; Song, S.; Suh, H.; Park, S.; Kim, J. Y. *Phys. Chem. Chem. Phys.* **2010**, *23*, 2759–2763.
(24) Kim, G. H.; Song, H. K.; Kim, J. Y. *Sol. Energy Mater. Sol. Cells* **2010**, *95*, 1119–1122.
(25) Park, H. J.; Lee, T. W.; Chin, B. D.; Wang, D. H.; Park, O. O. *Macromol. Rapid Commun.* **2010**, *31*, 2095–2108.